Optical Materials 35 (2013) 2257–2260

Contents lists available at SciVerse ScienceDirect

Optical Materials

journal homepage: www.elsevier.com/locate/optmat

Proton or helium ion beam written channel waveguides in Nd:YAG ceramics

Yicun Yao [a], Chao Zhang [a,c], Sudheer Kumar Vanga [b], A.A. Bettiol [b], Feng Chen [a,*]

[a] School of Physics, State Key Laboratory of Crystal Materials and Key Laboratory of Particle Physics and Particle Irradiation (MOE), Shandong University, Jinan 250100, China
[b] Centre for Ion Beam Applications, Department of Physics, National University of Singapore, Singapore
[c] Homer L. Dodge Department of Physics and Astronomy, University of Oklahoma, Norman, OK 73019, USA

ARTICLE INFO

Article history:
Received 28 February 2013
Received in revised form 2 June 2013
Accepted 5 June 2013
Available online 29 June 2013

Keywords:
Channel waveguide
Proton beam writing
He ion beam writing
Nd:YAG ceramics

ABSTRACT

We report on the fabrication of channel waveguides in Nd:YAG ceramics, using either focused proton beam writing (PBW) or He beam writing (HeBW) techniques. Energies of ions used in the writing process were at 1 MeV and 2 MeV, respectively, with different writing fluence. High quality channel waveguides were produced in both H^+ and He^+ implanted regions. Characteristics of the waveguides were explored, and refractive index distribution of the waveguide was reconstructed.

1. Introduction

Optical waveguide is one of the basic components in integrated optics and optoelectronics [1,2]. In such structures, light propagation is confined to very small volumes and can reach high optical intensities, making use of the total internal reflection principle. Compared with one dimensional waveguides such as planar or slab, channel waveguides restrict light propagation in two dimensions. As a result, the optical intensities within the channel waveguide regions can reach much higher levels compared to the bulk samples [3–6]. Consequently, the nonlinearities or laser actions in such waveguides may be more efficient than those in bulk materials. Moreover, the components based on channel waveguides can be interconnected with optical fibers for telecommunication application, in which waveguides are often used as amplifiers, signal switches, modulators, etc. [7,8].

Proton beam writing (PBW) and He beam writing (HeBW) are advanced techniques which are used for the inscription of three-dimensional (3D) structures in diverse materials [9–12]. In such processes, ion beams (H^+ and He^+) with energy of 1–3 MeV are focused to micro- or submicron-scales [13]. Because of the energy and momentum mismatch between the injecting ions and electrons in the target materials, the ions will maintain a straight path and cause little proximity effect as energy obtained by secondary electrons will be low [14]. Compared to traditional ion implantation techniques to form channel waveguides, PBW and HeBW are maskless, direct fabricating methods. This makes it an efficient technology to fabricate 3D high aspect ratio nanostructures in various materials [15–18]. In recent years, PBW has been successfully used to produce channel waveguides in a few materials, including organic polymers, glasses, silicon, and diamond [19–23]. More recently, our group have reported on the fabrication of channel waveguides in laser crystals, i.e., Nd:YAG, and Nd:GGG, using PBW technique, and continuous wave (cw) waveguide lasers with highly symmetric modes have been realized [24,25].

Neodymium-doped yttrium aluminum garnet (Nd:YAG) ceramic is an outstanding laser material that has emerged in recent years [26,27]. It shows several advantages over their crystalline partners while retaining the outstanding fluorescence properties of neodymium ions [28]. In this paper, PBW and HeBW methods were used to fabricate channel waveguides in Nd:YAG ceramics, and their waveguiding properties were characterized.

2. Experimental methods

In this work, two optically polished Nd:YAG (doped with 1 at.% Nd^{3+} ions) ceramics were used. Waveguides were written using focused H^+ and He^+ ion beams. The H^+ writing sample was cut into dimensions of $10(x) \times 9(y) \times 2(z)$ mm^3, and the He^+ written sample was cut into a similar dimensions of $10(x) \times 7(y) \times 2(z)$ mm^3. In both the samples, the writing process was carried out x–y plane of the samples. The PBW and HeBW implantation processes were carried out by using the facilities at the Centre for Ion Beam

* Corresponding author. Tel.: +86 531 88363007.
E-mail address: drfchen@sdu.edu.cn (F. Chen).

0925-3467/$ - see front matter © 2013 Elsevier B.V. All rights reserved.
http://dx.doi.org/10.1016/j.optmat.2013.06.011

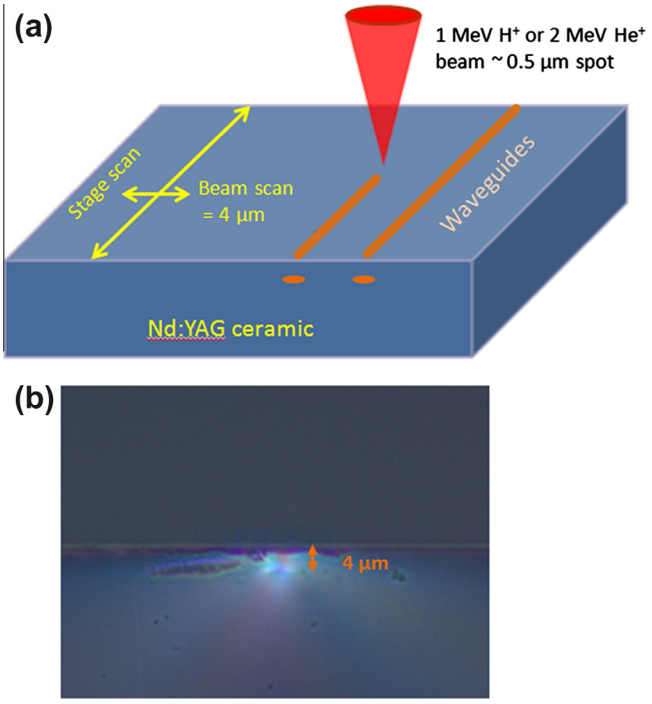

Fig. 1. (a) Schematic of the H^+ and He^+ beam writing process of Nd:YAG ceramic. (b) Metalloscope image of the end-face of the sample (He^+ implanted waveguide with fluence of 2.5×10^{15} ions/cm^2).

Applications, National University of Singapore. The H^+ and He^+ beams used had energy of 1 MeV and 2 MeV respectively, both focused down to spots with diameter less than 1 μm. During the process, samples were mounted on a motorized stage (Exfo inchworm stage, moving linearly at different speeds), and the ion beam was magnetically scanned over a distance of 4 μm in a perpendicular direction to the beam pathway on the x–y faces. The irradiation process is shown in Fig. 1a. Different writing fluences of 1×10^{16}, 1.5×10^{16}, 2×10^{16}, 3×10^{16} cm^{-2} for H^+ beam writing, and 2.5×10^{15}, 5×10^{15}, 1×10^{16} cm^{-2} for He^+ beam writing, were employed. The formed channel waveguides were along the *y* axis of the wafers.

3. Results and discussion

The cross section of the formed waveguide (He^+ implanted waveguide with fluence of 2.5×10^{15} ions/cm^2) was observed under the polarized light using the metalloscope (Carl Zeiss, Axio Imager), as shown in Fig. 1b. One can clearly see the light guiding inside the ceramic. The location of the guide is at a depth of about 4 μm. Similar metalloscope images were captured for other waveguides (pictures not shown here for the sake of brevity).

To further explore the characteristics of the formed waveguides, a conventional end-face coupling optical system was used to measure the modal profiles of the waveguides at wavelength of 632.8 nm by using a He–Ne laser. The modal profiles obtained are shown in Fig. 2. As one can see, for all fluences chosen here, single-mode buried channel waveguides were formed at the end of ion beam trajectories. And light propagation was confined for both TE and TM modes. Waveguides fabricated using the H^+ beam showed a decrease in contrast of light intensity between waveguide region and the bulk with increasing fluence, this suggests that a decrease of waveguide quality occurred. While for the waveguides fabricated using the He^+ beam writing one, high quality waveguides were observed for all fluences ranging from 2.5×10^{15} to 1×10^{16} cm^{-2}.

The defect (defect per atom, DPA) and the injecting ions concentration distributions, caused by the 1 MeV H^+ and He^+ beams in Nd:YAG ceramic, are calculated by utilizing the commercial software SRIM 2010 code [29], as shown in Fig. 3. Fluences used in the calculation are both set as 1×10^{16} cm^{-2}. As one can see, the projected average ion ranges (R_p) are about 10 μm and 4.3 μm, for the H^+ and He^+ situations respectively, which suggest the locations of formed waveguides. The result is also self-consistent with the microphotograph shown in Fig. 1b. The ion-induced damage is very low (in orders of 10^{-2}), which suggest that minor modification on the original lattices of Nd:YAG ceramic. In such cases, nuclear collision is the main factor for the local refractive index increment, either because of the local modification of the bond polarizability or the local density at the nuclear collision volume. We also esti-

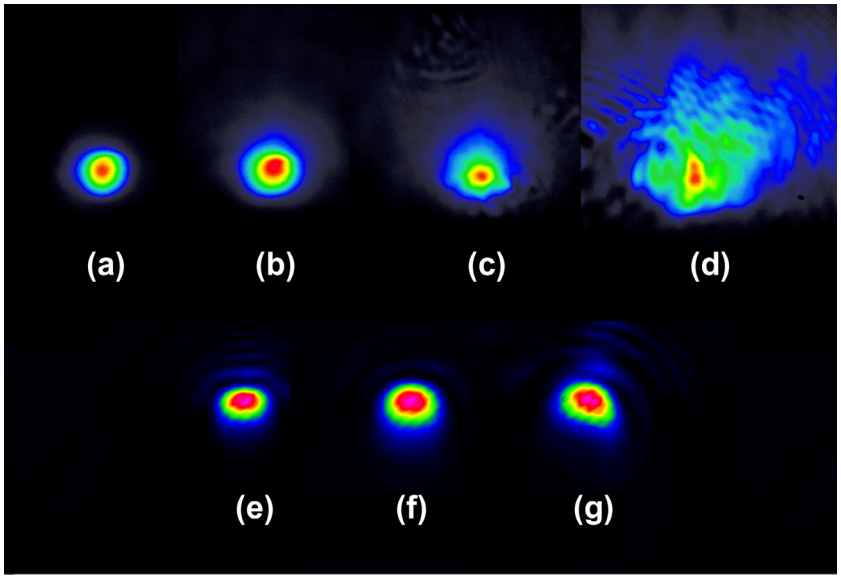

Fig. 2. (a–d) End-face modal profiles obtained for waveguides formed using proton beam writing, with fluences at 1×10^{16}, 1.5×10^{16}, 2×10^{16}, 3×10^{16} cm^{-2} respectively. (e–g) Modal profiles of helium beam writing induced waveguides, with fluences at 2.5×10^{15}, 5×10^{15}, 1×10^{16} cm^{-2}, respectively.

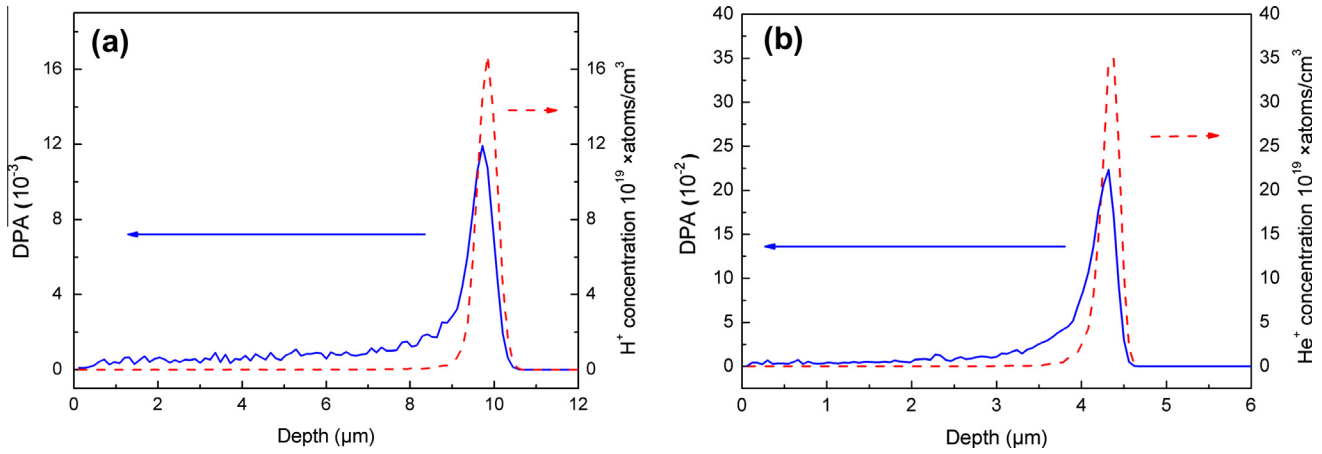

Fig. 3. Defect per atom (DPA) (blue solid line) and ion range (red dashed line) profiles of injecting ion beams, both calculated with fluence of 1×10^{16} cm^{-2}, based on SRIM calculation. (a) indicates the 1 MeV PBW situation and (b) for the 2 MeV HeBW one. (For interpretation of the references to color in this figure legend, the reader is referred to the web version of this article.)

mated the propagation loss of the waveguide, that was implanted with the 1×10^{16} cm^{-2} H^+, using the Fabry–Perot method. Results show a loss of 1.5–2 dB/cm (after annealing at 200 °C for 0.5 h). This is lower than previously reported waveguides in Nd:YAG crystal [23].

The refractive index change induced by the writing beam was estimated, by measuring the numerical aperture (NA) of the channel waveguide. The maximum of index increase was determined by the formula

$$\Delta n = \frac{\sin^2 \theta_m}{2n} \quad (1)$$

where n is the related refractive index of the bulk Nd:YAG ceramic, and θ_m is the maximum incident angle at which no transmitted guiding light occurring inside the waveguide [30]. After calculation, the maximum increase in refractive index obtained was about 1.4×10^{-3}, for the He^+ writing waveguide with fluence of 2.5×10^{15} cm^{-2}. Based on this, and considering the end-face modal profile, we tried to reconstruct the refractive index distribution to describe this type of PBW and HeBW induced channel waveguides. The reconstruction work was carried out on the same He^+ irradiation waveguide. The reconstructed refractive index profile is shown in Fig. 4c. Based on the index distribution, we calculated the modal profile of waveguide, using the finite-difference beam propagation method (FD-BPM) through the commercial software Rsoft BeamPROP©. By comparing Fig. 4a and b, one can see that the simulated profile is in good agreement with the experimental one, which suggests that the reconstruction of the refractive index distribution is reasonable.

4. Conclusion

We have reported on the fabrication of buried channel waveguides in Nd:YAG ceramic, using PBW and HeBW techniques, using different irradiation fluences. Channel waveguides were produced

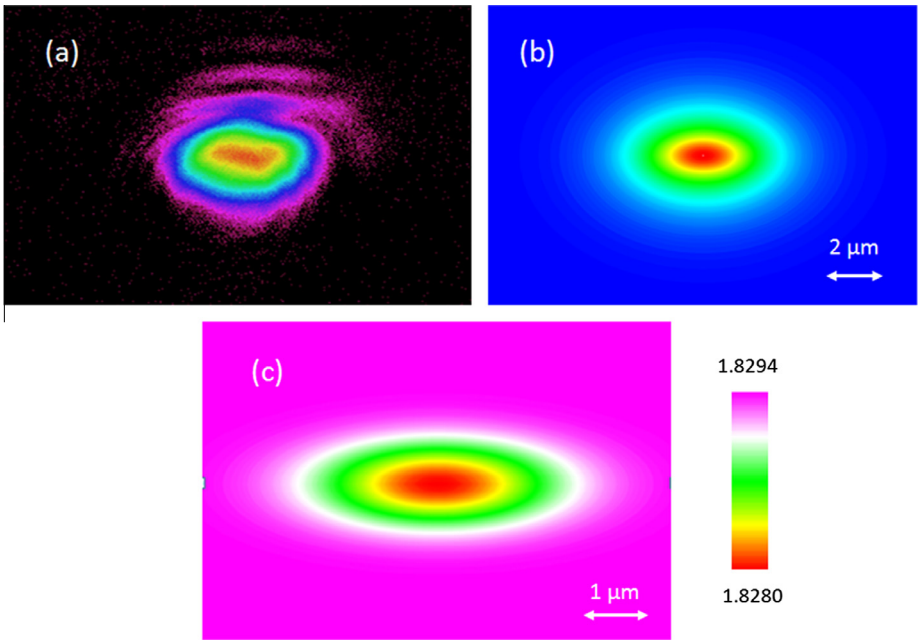

Fig. 4. (a) Measured and (b) calculated modal profiles of the fundamental mode at wavelength of 632.8 nm, corresponding to the Nd:YAG ceramic channel waveguide produced by 1 MeV HeBW at fluence of 2.5×10^{15} cm^{-2}. (c) Reconstructed refractive index profile.

in the end of ion trajectories, both for the proton and helium ion writing cases, among the fluence of 10^{-15} to 10^{-16} cm^{-2}. Metalloscope images were captured for the He^+ writing waveguide, showing a depth of about 4 μm from the surface, which is consistent with the SRIM calculation. Based on the He^+ writing waveguide with fluence at 2.5×10^{15} cm^{-2}, a refractive index distribution was reconstructed, giving a maximum change in refractive index of 1.4×10^{-3}. The calculated modal profile was in good agreement with the experiment, suggesting that the index distribution is reasonable.

Acknowledgments

The work is supported by the National Natural Science Foundation of China (No. 10925524), and the 973 Project (No. 2010CB832906) of China.

References

[1] J.I. Mackenzie, IEEE J. Sel. Top. Quantum Electron 13 (2007) 626–637.
[2] F. Chen, Laser Photon. Rev. 6 (2012) 622–640.
[3] H. Hu, F. Lu, X.L. Wang, F. Chen, K.M. Wang, Opt. Express 20 (2012) 21114–21118.
[4] E.J. Murphy, Integrated Optical Circuits and Component: Design and Applications, Marcel Dekker, New York, 1999.
[5] K.van. Dalfsen, S. Aravazhi, C. Grivas, S.M. García-Blanco, M. Pollnau, Opt. Lett. 37 (2012) 887–889.
[6] Y.Y. Ren, N.N. Dong, J. Macdonald, F. Chen, H.J. Zhang, A.K. Kar, Opt. Express 20 (2012) 1969–1974.
[7] G.I. Stegeman, C.T. Seaton, J. Appl. Phys. 58 (1985) R57.
[8] Y. Tan, F. Chen, J.R. Vazquez de Aldana, G.A. Torchia, A. Benayas, D. Jaque, Appl. Phys. Lett. 97 (2010) 031119.
[9] F. Watt, M.B.H. Breese, A.A. Bettiol, J.A. van Kan, Mater. Today 10 (2007) 20–29.
[10] R. Won, Nat. Photon. 74 (2011) 1038.
[11] P. Olivero, S. Rubanov, P. Reichart, B.C. Gibson, S.T. Huntington, J. Rabeau, A.D. Greentree, J. Salzman, D. Moore, D. Jamieson, S. Prawer, Adv. Mater. 17 (2005) 2427–2430.
[12] S. Lagomarsino, P. Olivero, F. Bosia, M. Vannoni, S. Calusi, L. Giuntini, M. Massi, Phys. Rev. Lett. 105 (2010) 233903.
[13] J.A. van Kan, P. Matar, A. Baysic de Vera, X. Chen, A.A. Bettiol, F. Watt, Nucl. Instrum. Methods A 645 (2011) 113–115.
[14] H.J. Whitlow, M.L. Ng, V. Auželytė, I. Maximov, L. Montelius, J.A. van Kan, A.A. Bettiol, F. Watt, Nanotechnology 15 (2004) 223–226.
[15] J.A. van Kan, P.G. Shao, Y.H. Wang, P. Malar, Microsyst. Technol. 17 (2011) 1519–1527.
[16] I. Rajta, S.Z. Szilasi, P. Fürjes, Z. Fekete, C. Dücső, Nucl. Instrum. Methods B 267 (2009) 2292–2295.
[17] K. Ansari, J.A. van Kan, A.A. Bettiol, F. Watt, Appl. Phys. Lett. 85 (2004) 476–478.
[18] M. Sarkar, N. Shukla, N. Banerji, Y.N. Mohapatra, Appl. Surf. Sci. 258 (2012) 4195–4198.
[19] A.A. Bettiol, S. Venugopal Rao, T.C. Sum, J.A. van Kan, F. Watt, J. Cryst. Growth 288 (2006) 209–212.
[20] T.C. Sum, A.A. Bettiol, H.L. Seng, I. Rajta, J.A. van Kan, F. Watt, Nucl. Instru. Methods B 210 (2003) 266–271.
[21] T.C. Sum, A.A. Bettiol, J.A. van Kan, F. Watt, E.Y.B. Pun, K.K. Tung, Appl. Phys. Lett. 83 (2003) 1707–1709.
[22] A.A. Bettiol, S. Venugopal Rao, E.J. Teo, J.A. van Kan, F. Watt, Appl. Phys. Lett. 88 (2006) 171106.
[23] A. Benayas, D. Jaque, Y.C. Yao, F. Chen, A.A. Bettiol, A. Rodenas, A.K. Kar, Opt. Lett. 35 (2010) 3898–3900.
[24] Y.C. Yao, Y. Tan, N.N. Dong, F. Chen, A.A. Bettiol, Opt. Express 18 (2010) 24516–24521.
[25] Y.C. Yao, N.N. Dong, F. Chen, S.K. Vanga, A.A. Bettiol, Opt. Lett. 36 (2011) 4173–4175.
[26] T. Calmano, A.G. Paschke, J. Siebenmorgen, S.T. Fredrich-Thornton, H. Yagi, K. Petermann, G. Huber, Appl. Phys. B 103 (2011) 1–4.
[27] Y. Tan, C. Zhang, F. Chen, F.Q. Liu, D. Jaque, Q.M. Lu, Appl. Phys. B 103 (2011) 837–840.
[28] H.L. Liu, Y.C. Jia, J.R. Vázquez de Aldana, D. Jaque, F. Chen, Opt. Express 20 (2012) 18620–18629.
[29] J.F. Ziegler, computer code, SRIM. <http://www.srim.org>.
[30] N.N. Dong, Y.C. Yao, Y.C. Jia, F. Chen, S.K. Vanga, A.A. Bettiol, Q.M. Lu, Opt. Mater. 35 (2012) 184–186.